Journal of Solid State Chemistry 182 (2009) 790–798

Contents lists available at ScienceDirect

Journal of Solid State Chemistry

journal homepage: www.elsevier.com/locate/jssc

New synthesis of nanopowders of proton conducting materials. A route to densified proton ceramics

Zohreh Khani [a], Mélanie Taillades-Jacquin [a], Gilles Taillades [a], Mathieu Marrony [b], Deborah J. Jones [a,*], Jacques Rozière [a]

[a] Institut Charles Gerhardt Montpellier, UMR 5253, Laboratoire des Agrégats, Interfaces et Matériaux pour l'Energie, Université Montpellier II, 34095 Montpellier, France
[b] European Institute for Energy Research, Emmy-Noether Strasse 11, 76131 Karlsruhe, Germany

ARTICLE INFO

Article history:
Received 23 October 2008
Received in revised form
17 December 2008
Accepted 23 December 2008
Available online 6 January 2009

Keywords:
Barium yttrium cerate
Barium yttrium zirconate
Nanopowders
Reverse micelles
Acrylate hydrogelation
High density ceramic membrane
Proton conductivity
Proton ceramic fuel cell

ABSTRACT

Low temperature routes have been developed for the preparation of $BaCe_{0.9}Y_{0.1}O_{2.95}$ (BCY10) and $BaZr_{0.9}Y_{0.1}O_{2.95}$ (BZY10) in the form of nanoparticulate powders for use after densification as ceramic membranes for a proton ceramic fuel cell. These methods make use on the one hand of the chelation of metal (II), (III) and (IV) ions by acrylates (hydrogelation route) and on the other of the destabilisation and precipitation of micro-emulsions. Both routes lead to single phase yttrium doped barium cerate or zirconate perovskites, as observed by X-ray diffraction, after thermal treatment at 900 °C for 4 h for BCY10 and 800 °C for BZY10. These temperatures, lower than those usually used for preparation of barium cerate or zirconate, lead to oxide nanoparticles of size <40 nm. Dense ceramics (⩾95%) are obtained by sintering BCY10 pellets at 1350 °C and BZY10 pellets at 1500 °C for 10 h. The water uptake of compacted samples at 500 °C is 0.14 wt% for BCY10 and 0.26 wt% for BZY10. Total conductivities in the range 300–600 °C were determined using impedance spectroscopy in a humidified nitrogen atmosphere. The total conductivity was 1.8×10^{-2} S/cm for BCY10 and 2×10^{-3} S/cm for BZY10 at 600 °C. The smallest perovskite nanoparticles and highest conductivities were obtained by hydrogelation of precursor barium, zirconium, cerium and yttrium acrylates.

1. Introduction

Proton conduction of perovskite-type oxides was described by Iwahara [1] in 1981 and since then aliovalent metal ion doped barium cerate and barium zirconate perovskites have been widely studied. Rare earth doped barium cerate exhibits higher proton conductivity than doped barium zirconate in the same conditions, but is less chemically inert in air, since carbonate formation tends to occur by reaction with carbon dioxide [2]. The literature provides some variation in the conductivity values of rare earth doped barium cerates and zirconates, depending on the preparative method used for the material, its capacity for water uptake, and the experimental conditions used in conductivity determination. Thus the conductivity of 10% yttrium doped barium cerate has been variously reported in the range between 10^{-4} and 10^{-2} S/cm at temperatures of 300–600 °C [3–6], while that of yttrium–barium zirconate has been described in an even broader range of 10^{-6}–10^{-3} S/cm at the same temperatures [6–11]. The higher value range of these conductivity values is sufficient for energy conversion applications, and these materials hold promise for use as solid electrolytes in proton ceramic fuel cells (PCFC) operating in the temperature range between that of proton exchange membrane and solid oxide fuel cells (PEMFC, SOFC), in particular between 400 and 600 °C. At this intermediate temperature, non-precious metal catalysts and oxide-type catalyst supports and electrode materials can be used, while the problem of thermal ageing of SOFC components is avoided to some extent.

Perovskite rare earth doped barium cerate and zirconate are conventionally prepared by solid state reaction from carbonate or oxide precursors. In addition, a large variety of wet chemistry methods have been employed such as co-precipitation [12–15] modifications of the Pechini method [16,17], glycine–nitrate combustion [18–20], sol–gel synthesis [21,22], polyacrylamide gel process [23], use of molten salts [24,25] and hydrothermal syntheses [26,27]. All these methods present their advantages and disadvantages. Drawbacks include difficulty in controlling the rate of hydrolysis of different metal alkoxides in the sol–gel process, a non-homogeneous compositional distribution and agglomeration of particles prepared by co-precipitation, the thermodynamic instability of barium cerate in the molten salt reaction medium [28] and inhomogeneous particle size and irregular morphology in hydrothermal methods. On the other hand, a single phase material can be obtained at high synthesis temperatures (>1000 °C) which will result in a large particle size (>100 nm).

* Corresponding author. Fax: +33 467 143304.
E-mail address: Deborah.Jones@univ-montp2.fr (D.J. Jones).

0022-4596/$ - see front matter © 2008 Elsevier Inc. All rights reserved.
doi:10.1016/j.jssc.2008.12.020

Oxide particles of size in the nanometre range are essential for good sinterability, allowing the elaboration of well-densified perovskite membranes of high conductivity [29,30] in which grain boundary effects are minimised. In addition, the availability of sufficiently small particles opens up the possibility of using deposition techniques such as spray pyrolysis.

In this study we have developed, optimised and compared two methods for the preparation of yttrium doped barium cerate and zirconate: a reverse micellar process and a method making use of a polymerised complex via hydrogelation of metal acrylate salts. Previous studies [28,31–34] have demonstrated the efficiency of micro-emulsion synthesis to produce nanosize ceramic powders at low temperatures, but this route has not been used for preparation of protonic oxides. This method leads to homogenous nanoparticles and well-densified materials, but presents some shortcomings compared to the use of hydrogels prepared from metal acrylate precursors. Hydrogelation was described for preparation of electrode ceramics such as $La_{0.8}Sr_{0.2}MnO_3$ [35] but has never been adapted for the development of proton ceramic electrolytes. We also describe the structural, morphological, water uptake and proton conduction properties of BCY10 and BZY10 prepared using these routes.

2. Experimental section

2.1. Hydrogelation of acrylates

Metal acrylates were prepared from the corresponding acetates. All chemicals were purchased from Sigma-Aldrich. The 25.00 mmol of barium acetate were dissolved in 100 mL of deionised water and 50.00 mmol of acrylic acid were added to this solution. The mixture was refluxed for 1 h and then rotary evaporated to remove the solvent. The white precipitate that formed was dried under vacuum overnight. Elemental analysis calculated for $Ba(C_3H_3O_2)_2.(H_2O)$: 24.20% C, 2.60% H and 46.33% Ba. Found: 24.32% C, 2.57% H and 46.91% Ba. Infrared spectroscopy (IR) confirmed the presence of the acrylate group by an absorption band at 1638 cm^{-1}. The same procedure was followed using 12.5 mmol of zirconium acetate diluted in acetic acid (Zr: 15–16%), 16.6 mmol of cerium acetate and 16.6 mmol of yttrium acetate with 50.00 mmol of acrylic acid in order to obtain zirconyl, cerium and yttrium acrylates, respectively. Elemental analysis calculated for $ZrO(C_3H_3O_2)_2.(H_2O)$: 26.9% C, 2.9% H and 34.1% Zr. Found: 25.62% C, 2.87% H and 33.53% Zr. The acrylate group appeared as a band at 1637 cm^{-1} in IR. Elemental analysis calculated for $Ce(C_3H_3O_2)_3.(H_2O)$: 29.12% C, 2.97% H and 37.75% Ce. Found: 28.66% C, 2.88% H and 37.82% Ce, acrylate group at 1639 cm^{-1} in IR. Elemental analysis calculated for $Y(C_3H_3O_2)_3.(H_2O)$: 33.7% C, 3.4% H and 27.7% Y. Found: 32.92% C, 3.37% H and 26.83% Y, acrylate group at 1642 cm^{-1} in IR.

2.1.1. Synthesis of $BaCe_{0.9}Y_{0.1}O_{2.95}$ (BCY10)

The 0.9667 g (3.2 mmol) of barium acrylate was dissolved in 100 mL of deionised water and refluxed for 30 min. The 22.7 mL of NH_4OH were added to the solution, which was further refluxed for a few minutes, then 47 mL acrylic acid were added and the solution was refluxed overnight. The cerium and yttrium oxide precursors were also prepared using 1.035 g (2.8 mmol) of cerium acrylate, 19.52 mL of NH_4OH, 40.17 mL of acrylic acid and 0.098 g (0.03 mmol) of yttrium acrylate, 2.15 mL of NH_4OH and 4.42 mL of acrylic acid, respectively. Each of the three solutions was concentrated by rotary evaporation until viscous gels had formed. The cerium containing gel was then added to the barium containing gel with 50 mL deionised water and the solution was again rotary evaporated. The yttrium containing gel was added to this mixture with 100 mL of deionised water, the solution was refluxed overnight and the solvent was removed by rotary evaporation at the end of procedure. The final yellow viscous gel obtained was heated at 400 °C for 3 h and then at 900 °C for 4 h leading to BCY10 (0.95 g, 95%) yield.

2.1.2. Synthesis of $BaZr_{0.9}Y_{0.1}O_{2.95}$ (BZY10)

Barium acrylate (1.128 g, 3.8 mmol) was dissolved in 100 mL of deionised water and refluxed for 30 min. Then 25.7 mL of NH_4OH was added to the solution, which was refluxed for 15 min. The 46.3 mL acrylic acid was added slowly to the hot solution and the solution was refluxed overnight. Similarly, the zirconyl and yttrium precursors were prepared using 0.870 g (3.2 mmol) of zirconyl acrylate, 21.8 mL of NH_4OH, 39.4 mL of acrylic acid and 0.115 g (0.03 mmol) of yttrium acrylate, 2.5 mL of NH_4OH and 5.14 mL of acrylic acid. Each metal acrylate solution was then concentrated by rotary evaporation to give a viscous gel. The zirconyl containing gel was added to the barium containing gel with 50 mL deionised water and the solution was again concentrated by rotary evaporation. Next, the yttrium gel precursor was added to this mixture with 100 mL of deionised water and the solution was again refluxed overnight. Evaporating all the solvents leads to obtain a very viscous white gel which was heated at 400 °C for 3 h and then at 800 °C for 4 h to convert to BZY10 (0.96 g, 96%) yield.

2.2. Reverse micelles method

The nitrate salts of barium, cerium, yttrium and zirconium purchased from Sigma-Aldrich were used as the starting materials. A micro-emulsion system was used, including *n*-octane (Fluka) as the continuous oil phase, Brij 56 (Sigma-Aldrich) as the surfactant, 1-butanol (Fluka) as the co-surfactant and sodium hydroxide (Merck) as the precipitating agent.

2.2.1. Synthesis of BZY10

1.260 g (4.8 mmol) of $Ba(NO_3)_2$, 0.990 g (2.9 mmol) of $ZrO(NO_3)_2.6(H_2O)$ and 0.184 g (0.06 mmol) of $Y(NO_3)_3$ were dissolved in 40 mL of deionised water. This solution was then dispersed in a solution containing 80 mL of *n*-octane, 14.6 mL of 1-butanol, and 18 g of Brij 56 to form a micro-emulsion. A second micro-emulsion was prepared by adding a solution of 1.152 g of NaOH in 40 mL of deionised water in the same composition mixture of *n*-octane, 1-butanol and Brij 56. The micro-emulsions were stirred separately for 30 min and then the second micro-emulsion was added to the first, and mixed together using a magnetic stirrer for 1 h. A white precipitate formed, which was then separated by centrifuging at 8000 rpm for 15 min. Next, it was washed with methanol and freeze-dried. The product was ground and heated at 400 °C for 3 h and then at 800 °C for 4 h to obtain BZY10.

2.2.2. Synthesis of BCY10

The same procedure as for the synthesis of barium zirconate was applied to prepare 10% yttrium barium cerate. Stoichiometric amounts of $Ba(NO_3)_2$, $Ce(NO_3)_3.6(H_2O)$ and $Y(NO_3)_3$ were used as the starting materials. The as-processed yellow powders obtained were heated at 400 °C for 3 h and then at 900 °C for 4 h to convert to BCY10. All heating steps were carried out in ambient laboratory air.

Elemental analyses for were performed by the CNRS Service Central d'Analyses (Vernaison, France) using inductively coupled plasma atomic emission spectroscopy. Thermal analyses were performed in air using a Netzsch TG 439 thermobalance using a heating rate of 5 °C/min.

The morphology and the grain size of the as-prepared ternary oxide powders were studied using transmission electron microscopy (TEM, JEOL 1200 EX). The powders were ground and dispersed with ultra-sound treatment in ethanol before depositing on supports for observation.

Powders were ground and pressed into pellets (diameter 13 mm and thickness 0.8–0.9 mm) by cold pressing under 370 MPa at room temperature under vacuum. They were sintered at different temperatures for between 5 and 15 h with a ramp rate of 1.5 °C/min. The pellets were covered (alumina disc) to avoid any losses of barium during high temperature processing as this phenomenon would reduce the proton conductivities [36]. The density of the pellets was determined by measuring the geometric dimensions and weighing the pellets after sintering. The densified pellets were observed by scanning electronic microscopy (SEM, HITACHI 52600 N).

X-ray diffraction (XRD) was performed at room temperature with a Philips X'Pert diffractometer using Cu$K\alpha$ radiation on the powders obtained after calcination at the temperatures specified above for each of the preparation routes, and of sintered pellets, in order to confirm phase purity. XRD patterns were recorded in the 2θ range between 10° and 110° with a step size of 0.02° and a measuring time of 5 s at each step. The lattice parameters were refined using Jana 2000 programme.

To determine water uptake, well-densified pellets were first dried for 10 h at 900 °C under dry nitrogen, then cooled down to 500 °C. The samples were held at this temperature for 2 h in a dry nitrogen atmosphere. Moist nitrogen (3% H_2O, 97% N_2) was then passed over the sample by flowing N_2 (50 cm^3/min) through a water bubbler at room temperature. The water uptake at 500 °C was measured by recording the weight change with a thermobalance.

The conductivity of sintered pellets was determined by impedance spectra recorded between 300 and 600 °C in the 10 Hz–10 MHz frequency range using an HP4192A impedance analyser. Platinum electrodes were sputtered on the surfaces of polished samples. The sample was placed in a closed cell, wet nitrogen gas (bubbler at room temperature) was flowed through the cell and measurement was taken after stabilisation at each temperature.

3. Results and discussion

The Michael addition reaction by neutralisation of ammonia by acrylic acid in water leads to generation *in situ* of the hydrogen bonded 3,3′,3″-nitrilotripropionic acid [$N(CH_2CH_2CO_2H)_3$] which complexes the metal acrylates and forms a hydrogel in which the metal ions are homogeneously distributed [35,37]. This mixture is converted to the corresponding metal oxides by pyrolysis. The method presents many advantages such as homogeneity, control of stoichiometry, short heating times and temperatures, low cost and the production of uniform particles of size in the nanometre range. The efficiency and yield of the reactions are also considerable (yield >94%) which enables the preparation of adequate quantities of materials.

In the reverse micelle method, the system consists of two micro-emulsion dispersions containing the required salts in which the aqueous droplets are stabilised by the surfactant in an oil phase. On mixing and stirring the two micro-emulsions, collision and exchange between the micelles occurs, leading to precipitation of complex oxides as nanoparticles. The growth of the nanoparticles is limited by the physical interactions between the particle surface and the hydrophilic head groups of the surfactant molecules. This method has been used by Leonard et al. [34] to prepare a non-doped barium zirconate ceramic oxide, but a small quantity of ZrO_2 impurity was observed in the final product, possibly due to the use of a less well-adapted basic surfactant (cetyl trimethylammonium bromide). In the present work, many parameters were controlled and adjusted to obtain single phase yttrium doped materials. It was found that the choice of non-ionic surfactants in particular is a key factor in preventing the formation of secondary phase impurities. These surfactants such as Brij were found to be more appropriate than ionic surfactants of the trimethylammonium type. The micro-emulsion method requires a large quantity of organic solvents and extensive washing of the final precipitates to remove all solvents and surfactants. As a result, many syntheses may be required to obtain a sufficient quantity of materials and this is a disadvantage compared with the method based on hydrogelation of acrylates.

The thermal decomposition of BCY10 and BZY10 gel precursors obtained via the hydrogelation of acrylates route are similar, showing a weight loss profile that occurs in several steps (Fig. 1a). The first stage between 30 and 180 °C results from loss of the adsorbed and structural water from the precursor gel, and is accompanied by an endothermic peak at in the DTA curve (at 125 °C in the zirconate precursor, 140 °C in the cerate precursor). The following step between 200 and 400 °C is related to the combustion and decomposition of the ammonium acrylate and 3,3′,3″-nitrilotripropionic acid produced during the hydrogelation reaction, which is related to the peaks in the DSC curves at 230–240 °C and 330 °C, when polyacrylic acid is formed [35]. Crystallisation occurs above 400 °C and the mass remains constant for temperatures above 600 °C. The thermal decomposition of BCY10 and BZY10 powder precursors obtained by the reverse micelles synthesis method is given in Fig. 1b. The first

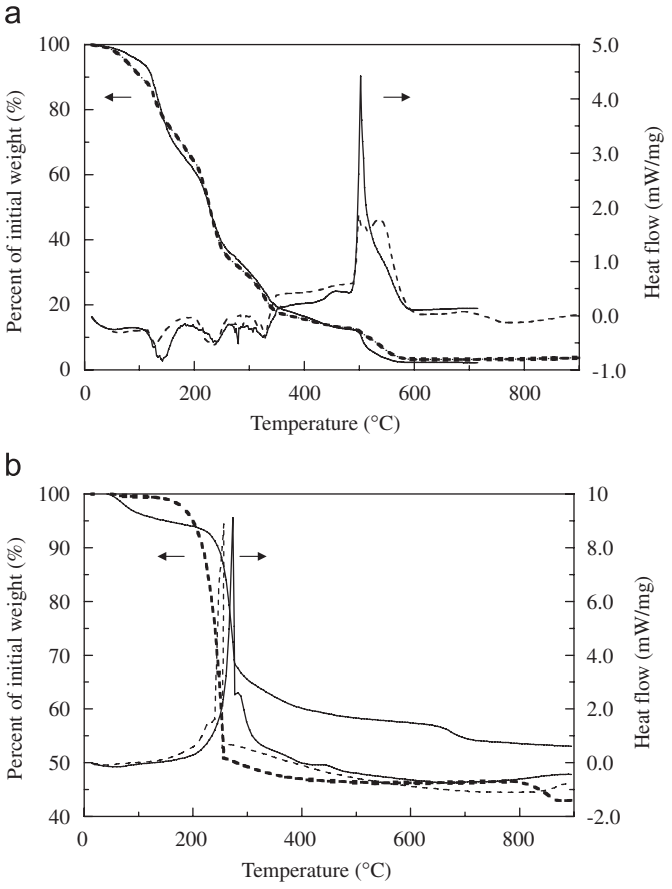

Fig. 1. Thermogravimetric and differential thermal analyses of BCY10 (full line) and BZY10 (dashed line) precursors prepared by: (a) hydrogelation of acrylates and (b) reverse micelles.

Table 1
Chemical analysis of sintered BCY10 and BZY10 prepared by hydrogelation of acrylates, using different quantities of barium acrylate.

Molar quantities of Ba:Ce:Y used in synthesis	Composition of sintered ternary oxide
1.00:0.90:0.10	$Ba_{0.96}Ce_{0.92}Y_{0.10}O_{2.95}$
1.05:0.90:0.10	$Ba_{1.00}Ce_{0.90}Y_{0.10}O_{2.95}$
1.10:0.90:0.10	$Ba_{1.05}Ce_{0.91}Y_{0.10}O_{2.95}$
1.00:0.90:0.10	$Ba_{0.96}Zr_{0.91}Y_{0.10}O_{2.95}$
1.05:0.90:0.10	$Ba_{1.00}Zr_{0.90}Y_{0.10}O_{2.95}$
1.10:0.90:0.10	$Ba_{1.05}Zr_{0.92}Y_{0.10}O_{2.95}$

Data reported as moles of cation per formula unit are the average of three analyses.

rapid weight loss from 30 °C to about 240 °C is related, to elimination of adsorbed and structural water, and solvents and surfactants (butanol, octane, methanol and Brij 56), the latter giving a strongly exothermic signal in the DTA (at 250 and 280 °C in the zirconate and cerate precursors, respectively). Crystallisation was observed around 700 °C for BZY10 and the mass remained constant above 800 °C. These temperatures are higher by about 100 °C for BCY10 in which the weight loss was complete after 900 °C. The association of all the thermal analytical data led us to develop a two stage calcination protocol, with a first step at 400 °C and a second at 800 °C for BZY10 and at 900 °C for BCY10.

Elemental analysis was carried out on all the samples prepared. The results showed that using the stoichiometric amount of barium in the method using hydrogelation of metal acrylates does not lead to the desired formulation. The resulting products contain a slightly insufficient quantity of barium. In subsequent preparations using this method, the small lack of barium was then compensated by adding an excess quantity (5%) of barium acrylate as starting material in the synthesis procedure (Table 1).

Transmission electron micrographs of BCY10 and BZY10 prepared by hydrogelation of acrylates and reverse micelle micro-emulsion after calcinations at 900 and 800 °C, respectively are shown in Figs. 2 and 3. The crystallite sizes are nanometric with homogeneous shape and size distributions in all cases. The particle size of BZY10 is smaller than that of BCY10, and the smallest particle sizes were obtained by hydrogelation of acrylates (Table 2). However, the particle size after calcination is <35 nm for BCY10 and <20 nm for BZY10 by both of the preparation methods.

XRD patterns of BCY10 powders calcined at 900 °C and BZY10 powders calcined at 800 °C for 4 h are shown in Figs. 4a and b, respectively. The patterns are in agreement with those previously reported [38–40] and confirm the purity of the crystalline product and presence of single perovskite phases. The space group of BCY10 is Pmcn with the lattice parameters $a = 6.2467(5)$Å, $b = 8.7684(5)$Å and $c = 6.2217(5)$Å. The space group of BZY10 is Pm $\bar{3}$m with $a = 4.2061(5)$Å. This value is close to that reported by Schober et al. [41] The grain size of the calcined products obtained by hydrogelation of acrylates was estimated using the Scherrer formula [42] as ~35 nm for BCY10 and ~22 nm for BZY10, very close to those directly observed in TEM.

The relative density of sintered pellets of BCY10 and BZY10 was determined for materials having undergone temperatures of sintering between 1300 and 1450 °C and between 1400 and 1600 °C, respectively. The results, as the average of measurement on three compacted pellets at each temperature and for a sintering time of 10 h (ramp of 1.5 °C/min) are presented in Fig. 5. As expected, the relative density (compacity) increases with the temperature of sintering in all cases. The compacity of the pellets prepared by hydrogelation of acrylates is slightly higher than that obtained on samples prepared via reverse micelles,

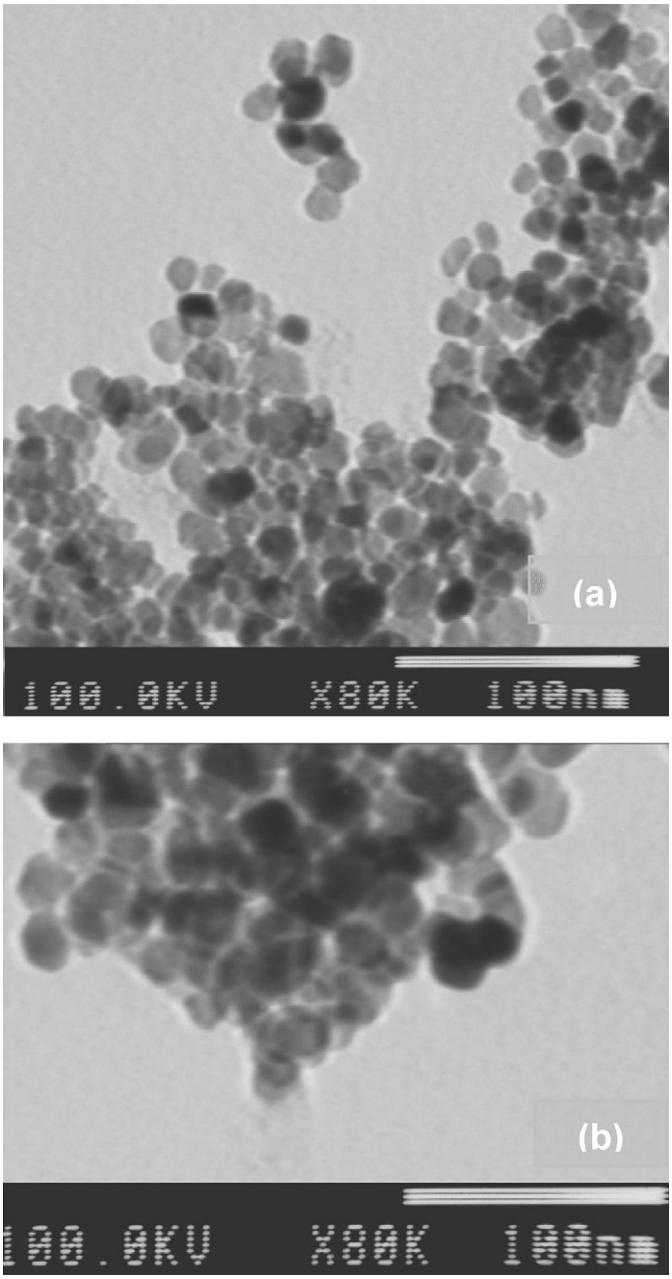

Fig. 2. TEM micrographs of BCY10 nanopowders obtained by hydrogelation of acrylates (a) and reverse micelles (b) after calcination at 900 °C.

probably a direct result of the smaller particle size obtained using the hydrogelation preparation route. The most highly densified samples (>93%) were obtained by sintering BCY10 pellets at 1350 °C and BZY10 pellets at 1500 °C for 10 h. SEM micrographs (Figs. 6–8) confirm a high degree of compaction. In addition, however, a porous surface layer is seen on the surface of BCY10 disc (Fig. 6) that was identified by XRD as cerium oxide, resulting from the decomposition of the BCY10 structure [43,44]. This surface layer can be removed by gentle abrasion on a SiC surface. Fig. 7 shows the dense core of a BCY10 pellet after abrasion, while Fig. 9 presents the diffraction pattern of a BCY10 pellet sintered at 1350 °C for 10 h before and after abrasion.

The amount of water that can be incorporated at 500 °C in BCY10 and BZY10 pellets compacted at ~95% was investigated using isothermal gravimetry. It is known from previous work [45]

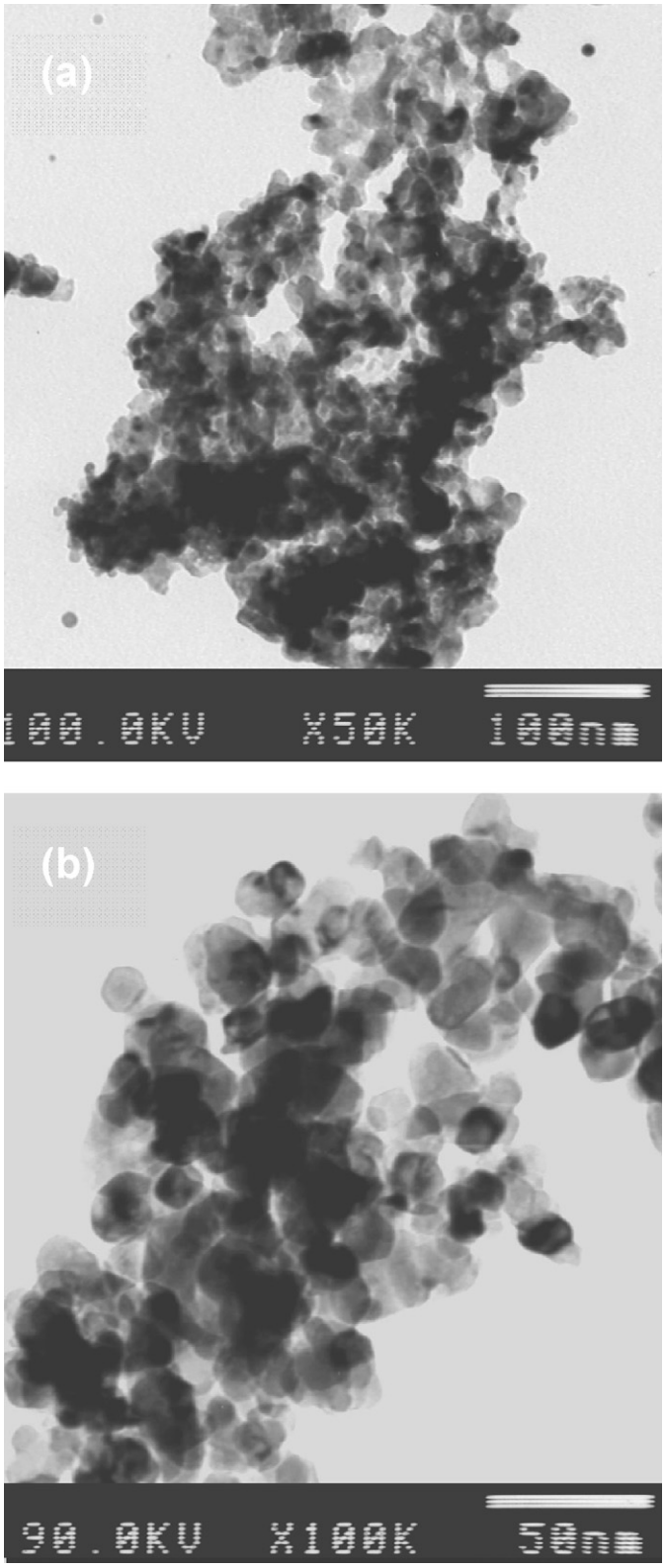

Fig. 3. TEM micrographs of BZY10 nanopowders obtained using hydrogelation of acrylates (a) and reverse micelles (b) after calcination at 800 °C.

that such ceramics have only p-type electronic conduction in hydrogen-free atmosphere, but that on introducing water vapour to the atmosphere, electronic conduction decreases and almost pure protonic conduction appears as a result of formation of hydroxyl groups at the oxygen vacancy sites in the perovskite

Table 2
Crystallite sizes of BCY10 and BZY10 prepared by reverse micelle and hydrogelation of acrylates methods.

Synthesis method	Particle size of BCY10 (nm)	Particle size of BZY10 (nm)
Reverse micelle	25–35	15–20
Hydrogelation of acrylates	20–30	10–15

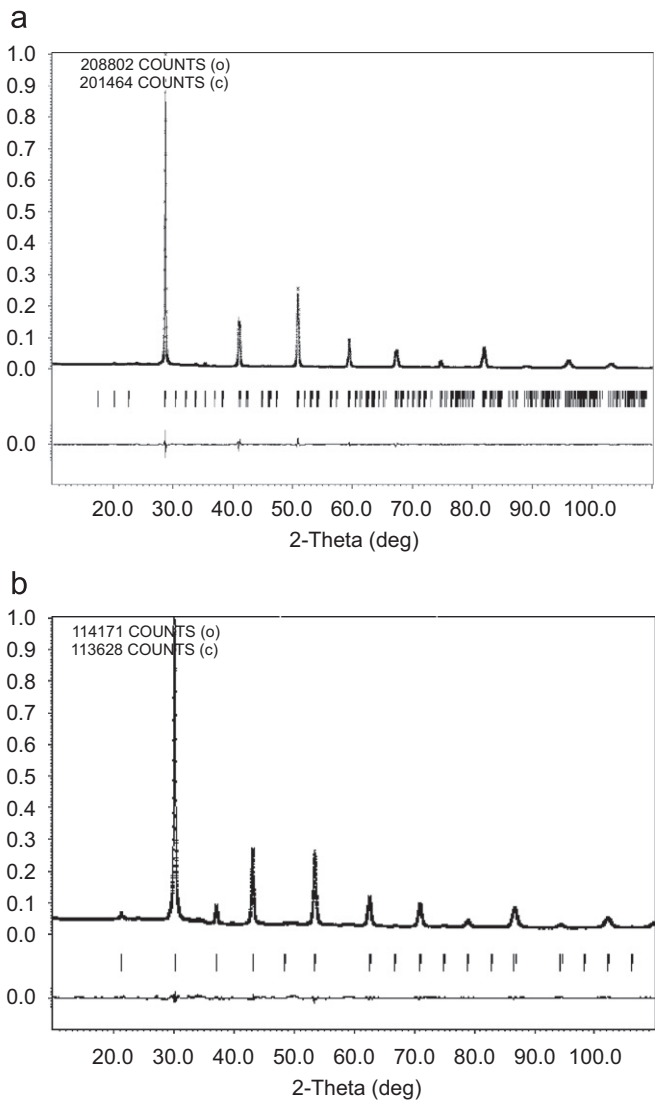

Fig. 4. X-ray diffraction pattern of powders obtained by hydrogelation of acrylates, BCY10 calcined at 900 °C (a) and BZY10 calcined at 800 °C (b).

structure. Neutron diffraction has been used to determine the location of the protons in the perovskite structure [46,47] and the principal feature of the proton transport mechanism has been established by quantum molecular dynamics simulations as being rotational diffusion of the protonic species and proton transfer towards a neighbouring oxide ion. In the present study, the samples were first dried at 900 °C under dry nitrogen and then cooled to 500 °C until the sample mass remained constant. Wet nitrogen was then flowed over the samples, causing a mass increase which corresponds to the water uptake by the sample. Once no further weight increase was observed, dry nitrogen was again introduced, leading to a weight loss approximately equal to the water uptake. For BCY10 pellets prepared through

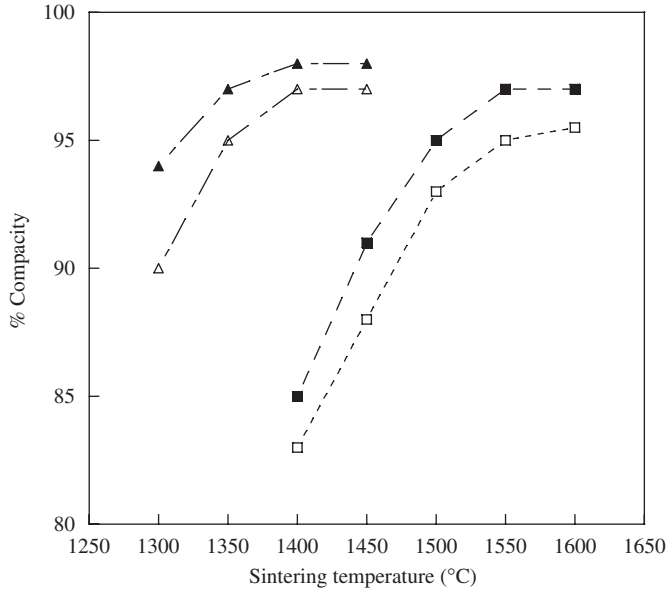

Fig. 5. Compacity of BCY10 prepared by ▲ hydrogelation of acrylates, Δ reverse micelles and BZY10 obtained via ■ hydrogelation of acrylates and □ reverse micelles as a function of sintering temperature for 10 h.

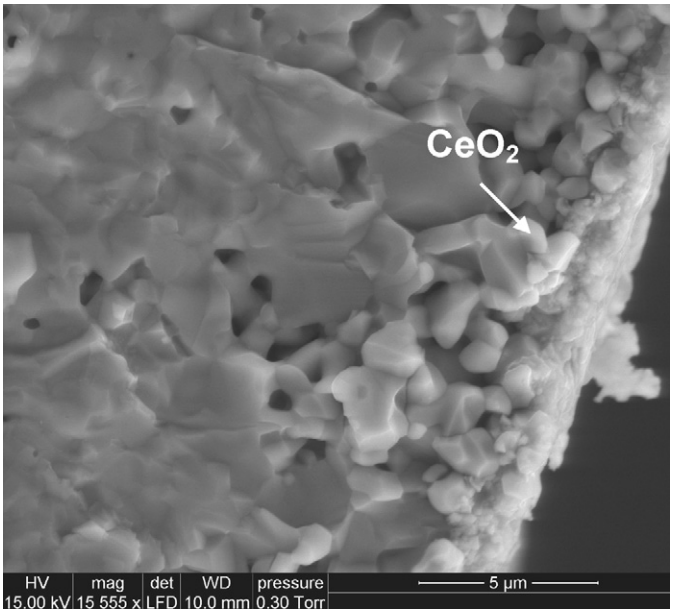

Fig. 6. SEM micrograph of BCY10 sintered for 10 h at 1350 °C (before abrasion).

hydrogelation of acrylates and reverse micelles, the increase in weight corresponding to water uptake is reached at 0.14 and 0.13 wt%, respectively.

The extent of water uptake is directly related to the oxygen vacancy concentration, each yttrium dopant being compensated by $\frac{1}{2}$ oxygen vacancy. The "water" content of BCY10 depends on the number of these vacancies ($\frac{1}{2}$ H_2O fill $\frac{1}{2}$ vacancy), and the theoretical maximum water uptake of BCY10 is 0.28 wt% which correspond to 100% of the nominal oxygen vacancies. In these experiments, the highest weight increase of 0.14% corresponds to 50% of vacancy filling. It was already observed that the maximum theoretical water uptake in rare earth doped cerates is never reached [48–50] and our results are in good agreement with the water incorporation study at different temperatures of Kruth on BCY10 [51], who described a weight increase of 0.13% at 500 °C. In

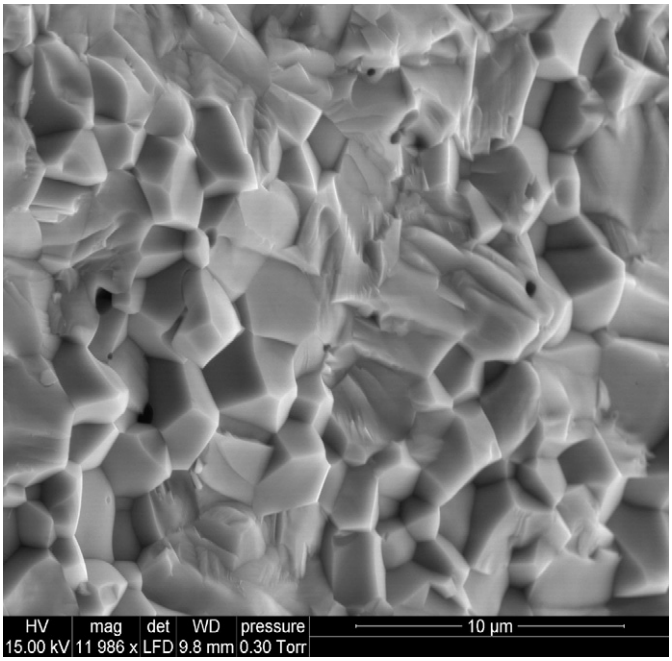

Fig. 7. SEM micrograph of fracture surface of BCY10 sintered for 10 h at 1350 °C (after abrasion).

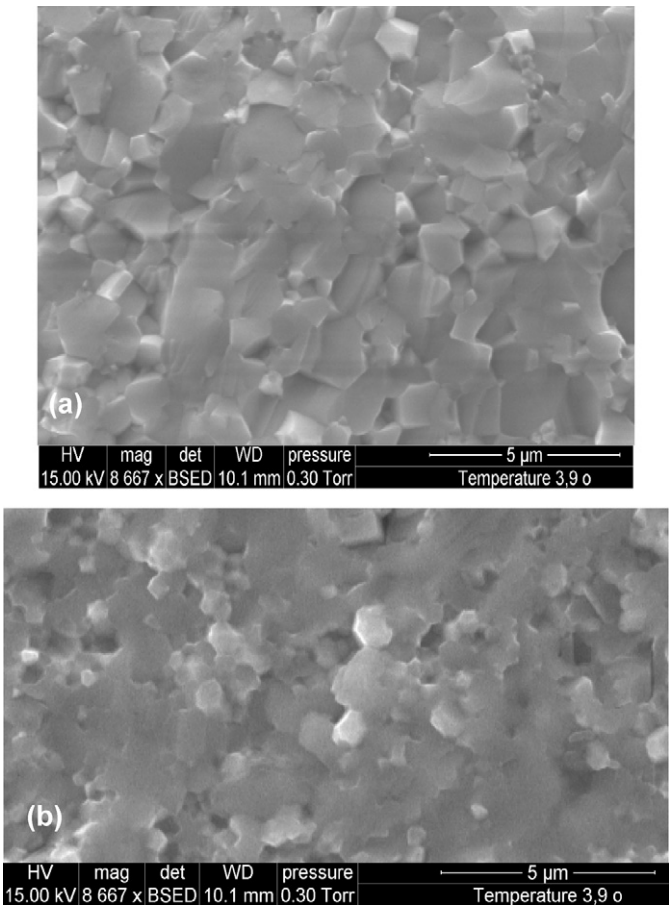

Fig. 8. SEM micrograph of fracture surface of BZY10 sintered for 10 h at 1500 °C obtained by hydrogelation of acrylates (a) and reverse micelles (b).

the present work, it was observed that up to 80% of the oxygen vacancies can be filled, but at lower temperature, 250 °C. The theoretical maximum water uptake of BZY10 is 0.32 wt%.

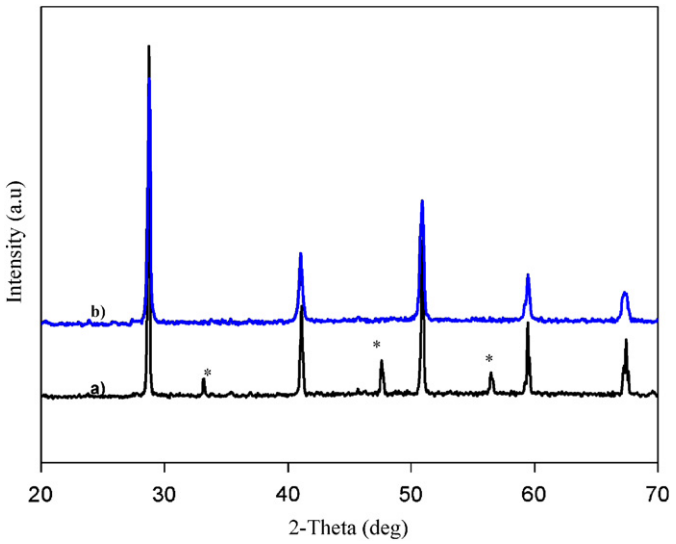

Fig. 9. X-ray diffraction pattern of BCY10 pellet prepared by use of reverse micelles, sintered at 1350 °C, before (a) and after (b) surface abrasion.

This experiment was repeated for the BZY10 pellets prepared by hydrogelation of acrylates and using reverse micelle microemulsion, and the results were 0.26 and 0.24 wt%, respectively, which correspond to about 81% and 75% of vacancy filling.

As described above, the relative density of BCY10 pellets sintered at 1350 °C prepared by hydrogelation of acrylates and reverse micelle reaches about 97% and 95%, respectively. The proton conductivity of these pellets was then determined between 300 and 600 °C and compared with that of a less-dense pellet with compacity of only 85%. An example of the impedance spectra recorded for BCY10 at 500 °C and BZY10 at 600 °C is given in Fig. 10. At these temperatures, semi-circles arising from bulk and grain boundary resistances cannot be resolved, and the total electrical resistance determined from the impedance spectra is the sum of $R_{total} = R_{bulk} + R_{grain\ boundary}$. The results are shown in Fig. 11 where it may be clearly seen that the conductivity is higher for the samples of higher compacity. At 500 °C, the total conductivity of BCY10 was 9.0×10^{-3} S/cm for the material prepared by hydrogelation of acrylates and 6.4×10^{-3} S/cm for that derived from the reverse micelles synthesis route. For the pellet densified only to 85%, this value is lower, 3.8×10^{-3} S/cm. The total resistance of the sample depends on the resistance of the grain boundary, which decreases with densification of the samples. These results confirm that densification step is a key factor in optimising the conduction properties of doped perovskite electrolytes For the pellets densified to >90%, even a difference of 2% in compacity leads to a significantly different conductivity.

The data obtained for conductivity of BCY10 are in agreement with although slightly higher than those reported by previous authors [3–6]. Comparison with the results of Coors and Readey [3] is most relevant, since these authors also determined the conductivity in the critical temperature range from 400–600 °C. The value of the activation energy E_a determined with Arrhenius equation for all samples is 0.48 ± 0.01 eV, which is typical of cerate-based proton ceramics.

For BZY10 pellets sintered at 1500 °C, the relative density is 95% for powders obtained by hydrogelation of acrylates and 93% for those obtained using reverse micelles. Their total conductivity at 600 °C is 2×10^{-3} S/cm and 1.8×10^{-3} S/cm, respectively. It is significantly lower, 5×10^{-4} S/cm, for the pellet densified up to 85%. As a result, in the case of BZY10, for the samples of compacity >90%, no difference in conductivity was observed while increasing the compacity from 85% to 93% has a considerable effect on

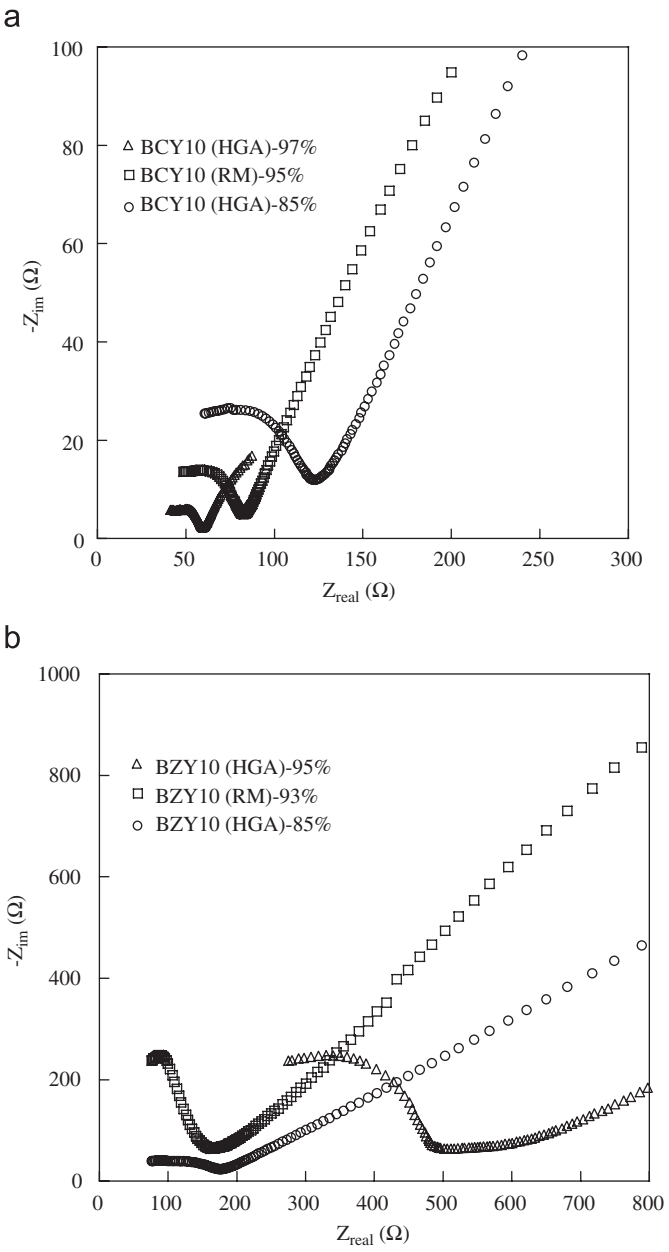

Fig. 10. Impedance spectra given by: (a) BCY10 at 500 °C for samples prepared by hydrogelation (HGA, compacity 97% and 85%) and reverse micelles (RM, compacity 95%) and (b) BZY10 at 600 °C for samples prepared by hydrogelation (compacity 95% and 85%) and reverse micelles (compacity 93%), under humidified N_2, Pt electrodes.

the conductivity (Fig. 12). The total conductivity of densified BZY10 prepared via nanopowder precursors (whether reverse micelle or hydrogelation of acrylates) are higher than most values previously reported for this composition [6–10], although is slightly lower than that of a 20 mol% yttria doped barium zirconate (4×10^{-3} S/cm) prepared by sol–gel processing and annealed at 1500 °C when a relative density of 99.4% was achieved [52]. The E_a determined from the Arrhenius equation for all samples is 0.69 ± 0.01 eV.

4. Conclusions

The objective of this research was to investigate the potential of two low temperature synthesis methods for the preparation of

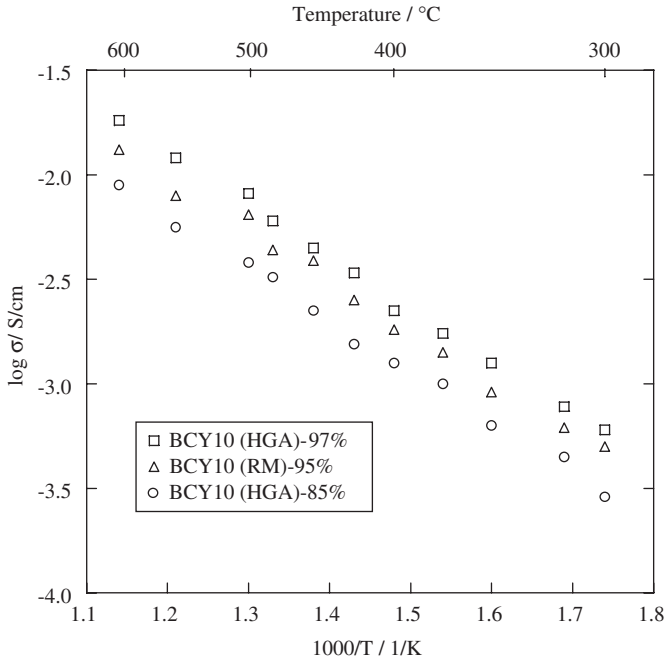

Fig. 11. Temperature dependence of total conductivities of BCY10 obtained by hydrogelation of acrylates (compacity 97% and 85%) and reverse micelles (compacity 95%).

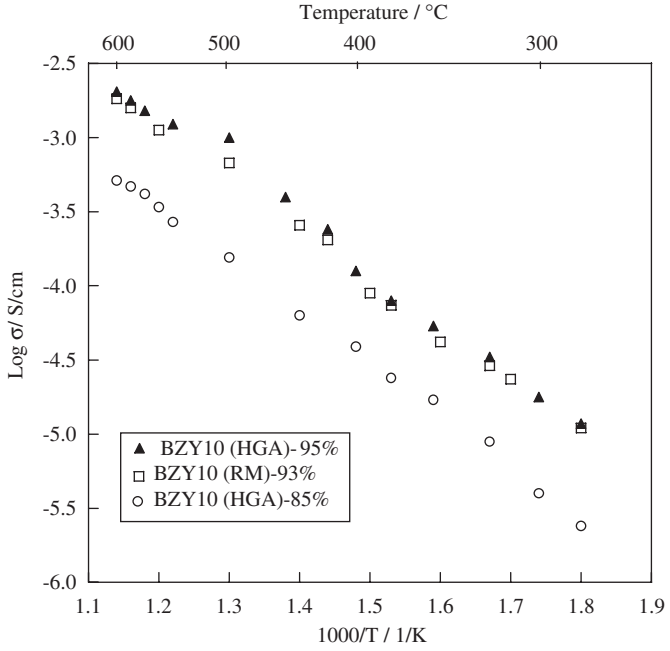

Fig. 12. Temperature dependence of total conductivities of BZY10 obtained by hydrogelation of acrylates (compacity 95% and 85%) and reverse micelles (compacity 93%).

proton conducting $BaCe_{0.9}Y_{0.1}O_{2.95}$ (BCY10) and $BaZr_{0.9}Y_{0.1}O_{2.95}$ (BZY10) in the form of nanopowders adapted for improved sinterability. The micro-emulsion and acrylate hydrogelation routes have not been used previously for the preparation of perovskite type proton conductors. The association of elemental analysis, transmission and scanning emission microscopies and X-ray diffraction provides converging results indicating the existence of nano-sized single phase crystallites. Sintered samples may be densified up to 93–98% of the theoretical values. The method making use of decomposition of a complex hydrogel provides smallest perovskite particles giving pellets of highest compacities. Dense pellets were easily hydrated in a water-containing atmosphere at 500 °C. Water uptake of BCY10 pellets from hydrogelation of acrylates and reverse micelles corresponds to 50% and 46% filled oxygen vacancies, while BZY10 pellets present 81% and 75% vacancy filling, respectively. The total conductivity of fully (>95%) and partially densified (85%) pellets of BCY10 and BZY10 determined by impedance spectroscopy confirms the positive effect of densification on each material. The total conductivity is 1.8×10^{-2} S/cm for BCY10 and 2.0×10^{-3} S/cm for BZY10 at 600 °C.

Such characteristics show that the hydrogelation of acrylates is an excellent approach to the preparation of proton conducting oxides for intermediate temperature fuel cells. The future work is dedicated to the integration of BCY10 and BZY10 in half-cells and a fuel cell, as well as the development of core-shell-type arrangements using nanopowder approaches.

Acknowledgments

Funding by the Plan d'Action National pour l'Hydrogène et les Piles à Combustible (PAN-H) de l'Agence Nationale de la Recherche under the Tectonic Project (ANR-05-PANH-015-03) is acknowledged. A bursary from the Agence de l'Environnement et de la Maîtrise de l'Energie (to Z.K.) is acknowledged with thanks.

References

[1] H. Iwahara, T. Esaka, H. Uchida, N. Maeda, Solid State Ionics 3–4 (1981) 359–363.
[2] K.H. Ryu, S.M. Haile, Solid State Ionics 125 (1999) 355–367.
[3] W.G. Coors, D.W. Readey, J. Am. Ceram. Soc. 85 (2002) 2637–2640.
[4] K.D. Kreuer, Annu. Rev. Mater. Res. 33 (2003) 333–359.
[5] N. Bonanos, B. Ellis, K.S. Knight, M.N. Mahmood, Solid State Ionics 35 (1989) 179–188.
[6] K. Katahira, Y. Kohchi, T. Shimura, H. Iwahara, Solid State Ionics 138 (2000) 91–98.
[7] V.P. Gorelov, V.B. Balakireva, Y.N. Kleshchev, V.P. Brusentsov, Transl. Neorg. Mater. 37 (2001) 535–538.
[8] R.C.T. Slade, S.D. Flint, N. Singh, Solid State Ionics 82 (1995) 135–141.
[9] C.D. Savaniu, J. Canales-Vazquez, J.T.S. Irvine, J. Mater. Chem. 15 (2005) 598–604.
[10] F.M.M. Snijkers, A. Buekenhoudt, J.J. Luyten, J. Cooymans, M. Mertens, Scr. Mater. 51 (2004) 1129–1134.
[11] H.G. Bohn, T. Schober, J. Am. Ceram. Soc. 83 (2000) 768–772.
[12] C.D. Sagel-Ransijn, A.J.A. Winnubst, A.J. Burggraaf, H. Verweij, J. Eur. Ceram. Soc. 16 (1996) 759–766.
[13] C.D. Sagel-Ransijn, A.J.A. Winnubst, B. Kerkwijk, A.J. Burggraaf, H. Verweij, J. Eur. Ceram. Soc. 17 (1997) 831–841.
[14] S.D. Flint, R.C.T. Slade, Solid State Ionics 77 (1995) 215–221.
[15] I.-H. Oh, S.-A. Hong, Y.-K. Sun, J. Mater. Sci. 32 (1997) 3177–3182.
[16] M.J. Scholten, J. Schoonman, J.C. van Miltenburg, H.A.J. Oonk, Solid State Ionics 61 (1993) 83–92.
[17] M.P. Pechini, US 3 330 697, 1967.
[18] L.A. Chick, L.R. Pederson, G.D. Maupin, J.L. Bates, L.E. Thomas, G.J. Exarhos, Mater. Lett. 10 (1990) 6–12.
[19] M. Jacquin, Y. Jing, A. Essoumhi, G. Taillades, D.J. Jones, J. Roziere, J. New Mater. Electrochem. Syst. 10 (2007) 243–248.
[20] G. Taillades, M. Jacquin, Z. Khani, D.J. Jones, M. Marrony, J. Roziere, ECS Transl. 7 (2007) 2291–2298.
[21] Y.-K. Sun, I.-H. Oh, S.-A. Hong, J. Mater. Sci. 31 (1996) 3617–3621.
[22] P.P. Phule, D.C. Grundy, Mater. Sci. Eng. B: Solid-State Mater. Adv. Technol. B 23 (1994) 29–35.
[23] A. Magrez, T. Schober, Solid State Ionics 175 (2004) 585–588.
[24] M. Descemond, C. Brodhag, F. Thevenot, B. Durand, M. Jebrouni, M. Roubin, J. Mater. Sci. 28 (1993) 2283–2288.
[25] S.F. Liu, W.T. Fu, Mater. Res. Bull. 36 (2001) 1505–1512.
[26] S. Komarneni, M.C. D'Arrigo, C. Leionelli, G.C. Pellacani, H. Katsuki, J. Am. Ceram. Soc. 81 (1998) 3041–3043.
[27] A.A. Athawale, M. Bapat, J. Metastable Nanocryst. Mater. 23 (2005) 3–6.
[28] J. Cai, K. Laubernds, F.S. Galasso, S.L. Suib, J. Liu, X.-F. Shen, E. Begge, H.R. Kunz, J.M. Fenton, J. Am. Ceram. Soc. 88 (2005) 2729–2735.
[29] W.H. Rhodes, J. Am. Ceram. Soc. 64 (1981) 19–22.

[30] C. Kleinlogel, L.J. Gauckler, Proc. Electrochem. Soc. 99–19 (1999) 225–232.
[31] A.J. Zarur, H.H. Hwu, J.Y. Ying, Langmuir 16 (2000) 3042–3049.
[32] L. Gao, H.C. Qiao, H.B. Qiu, D.S. Yan, J. Eur. Ceram. Soc. 16 (1996) 437–440.
[33] M.C. McLeod, R.S. McHenry, E.J. Beckman, C.B. Roberts, J. Phys. Chem. B 107 (2003) 2693–2700.
[34] K.J. Leonard, S. Sathyamurthy, M.P. Paranthaman, Chem. Mater. 17 (2005) 4010–4017.
[35] E.H. Walker Jr., A.W. Apblett, R. Walker, A. Zachary, Chem. Mater. 16 (2004) 5336–5343.
[36] D. Shima, S.M. Haile, Solid State Ionics 97 (1997) 443–455.
[37] E.H. Walker, J.W. Owens, M. Etienne, D. Walker, Mater. Res. Bull. 37 (2002) 1041–1050.
[38] K. Takeuchi, C.K. Loong, J.W. Richardson Jr., J. Guan, S.E. Dorris, U. Balachandran, Solid State Ionics 138 (2000) 63–77.
[39] K.S. Knight, M. Soar, N. Bonanos, J. Mater. Chem. 2 (1992) 709–712.
[40] K.S. Knight, Solid State Ionics 127 (2000) 43–48.
[41] T. Schober, H.G. Bohn, Solid State Ionics 127 (2000) 351–360.
[42] A. Taylor (Ed.), Chapman and Hall, London, 1942.
[43] N. Zakowsky, S. Williamson, J.T.S. Irvine, Solid State Ionics 176 (2005) 3019–3026.
[44] G. Ma, T. Shimura, H. Iwahara, Solid State Ionics 110 (1998) 103–110.
[45] H. Iwahara, H. Uchida, K. Ono, K. Ogaki, J. Electrochem. Soc. 135 (1988) 529–533.
[46] K.S. Knight, Solid State Ionics 145 (2001) 275–294.
[47] K.S. Knight, N. Bonanos, Mater. Res. Bull. 30 (1995) 347–356.
[48] H. Iwahara, Solid State Ionics 86–88 (1996) 9–15.
[49] F. Krug, T. Schober, T. Springer, Solid State Ionics 81 (1995) 111–118.
[50] K.D. Kreuer, Solid State Ionics 125 (1999) 285–302.
[51] A. Kruth, J.T.S. Irvine, Solid State Ionics 162–163 (2003) 83–91.
[52] R.B. Cervera, Y. Oyama, S. Miyoshi, K. Kobayashi, T. Yagi, S. Yamaguchi, Solid State Ionics 179 (2008) 236–242.